Journal of Coastal Research	28	4	745–759	West Palm Beach, Florida	July 2012

A Review of Potential Tsunami Impacts to the Suez Canal

Charles W. Finkl[†], Efim Pelinovsky[‡], and Richard B. Cathcart[§]

[†]Department of Geosciences
Charles E. Schmidt College of Science
Florida Atlantic University
Boca Raton, FL 33431, U.S.A.
and
Coastal Education & Research Foundation
West Palm Beach, FL 33411, U.S.A.
cfinkl@cerf-jcr.com

[‡]Department of Nonlinear Geophysical Processes
Institute of Applied Physics
Russian Academy of Sciences
46 Uljanov Street
Nizhny Novgorod, 603950, Russia

[§]Geographos
1300 West Olive Avenue, Suite M
Burbank, CA 91506, U.S.A.

www.cerf-jcr.org

www.JCRonline.org

ABSTRACT

Finkl, C.W.; Pelinovsky, E., and Cathcart, R.B., 2012. A review of potential tsunami impacts to the Suez Canal. *Journal of Coastal Research,* 28(4), 745–759. West Palm Beach (Florida), ISSN 0749-0208.

Tsunamis in the eastern Mediterranean and Red Seas, induced by earthquakes and/or volcanic activity, pose potential hazards to shipping and fixed harbor infrastructure within the Suez Canal. Potential vulnerabilities of the Suez Canal to possible tsunami impacts are reviewed by reference to geological, historical, archeoseismological, and anecdotal data. Tsunami catalogues and databases compiled by earlier researchers are perused to estimate potential return periods for tsunami events that could directly affect the Suez Canal and operational infrastructures. Analysis of these various records indicates a centurial return period, or multiples thereof, for long-wave repetition that could generally impact the Nile Delta, whereas numerical models indicate a multidecadal frequency. It is estimated that tsunami waves 2 m high would begin to break about 4 to 10 km down-canal, whereas a 10-m wave break would occur about 0.5 to 3 km into the Canal.

ADDITIONAL INDEX WORDS: *Coastal geohazards, seismic sea wave, tsunamigenesis, coastal erosion, coastal flooding, Mediterranean Sea, Red Sea, shore-protection structures.*

INTRODUCTION

The Suez Canal (Figure 1) is the most commercially utilized and the longest (160 km) excavated waterway in the world, rivaled only by the Panama Canal. The canal is an inland coastal ocean–connected saltwater body that links the Mediterranean Sea in the north with the Red Sea in the south (Fremaux and Volait, 2009). The north–south trending channel sits on a line of longitude at 32°18′15″ E across the Isthmus of Suez in Egypt (*cf.* Figure 1). Coordinates of the entrance on the Red Sea are 29°55′58.8″N, 32°33′54″E (at Port Tawfik near the city of Suez), while the Mediterranean Sea entrances are 31°16′8.4″N, 32°19′22.8″E (Port Said) and 31°13′48″N, 32°20′49.2″E (Port Fouad). The canal mostly transits a desert environment and is bounded by sand banks, except for the northern 60 km bordered by extensive wetlands.

Its commercial and military-strategic value provides immeasurable savings in vessel voyage distance, sailing time, and transport costs. The position of Earth's landmasses, coupled with patterns of market, production, and mining, converges maritime trade at the Suez Canal, making it a transportation chokepoint. In spite of the transportation bottleneck, the Suez Canal is ranked as a global infrastructure solution from a macroengineering perspective (Calon, 1994). By 2011, at least 50 ships were passing through the Suez Canal daily. That is, two ships enter the waterway every hour every day of the year, with approximately 25 ships floating in the channel at any one time during a 24-hour period.

Because the Suez Canal lies at sea level and is without sea locks, it is susceptible to flooding by long waves (*e.g.,* Stiros, 2007). Tsunamis could thus damage and disrupt the canal's vital international role by impacting structures that facilitate the mass distribution of goods, services, and information. Although it is not possible to completely protect the harbors at either end of the Suez Canal (*e.g.,* Ports Said and Fouad at its northern end and Ports Suez and Adabiya at its southern end) from widespread inundation, ingress of tsunamis into the canal *per se* could be mitigated by construction of controllable surge gates.

Limited hydrographic surveys constrain the accuracy of generalizations of the geohazard threat posed by future tsunamis to the main channel and nearby infrastructures. The extensive array of potentially impacted infrastructure includes a coast-parallel railroad, cross-canal bridges, tunnels, freshwater siphons, and a thermal power plant (Nassar, 1988). The specific fixed infrastructures of major significance include (1) the El Ferdan Railway Bridge (30.657° N, 32.334° E) with a span of 340 m, the longest swing bridge in the world, that was completed in 1963 and whose bridge piers can be eroded; (2) the 1063-m-long Ahmed Hamdi Tunnel (30°5′9″ N, 32°34′32″ E; Otsuka and Kamel, 1995) that has been passing vehicles under the Suez Canal since 1983, the entrance/exit of which can foreseeably be flooded by high levee-overtopping tsunami

DOI: 10.2112/JCOASTRES-D-12A-00002.1 received 22 January 2012; accepted in revision 22 January 2012.
Published Pre-print online 15 May 2012.

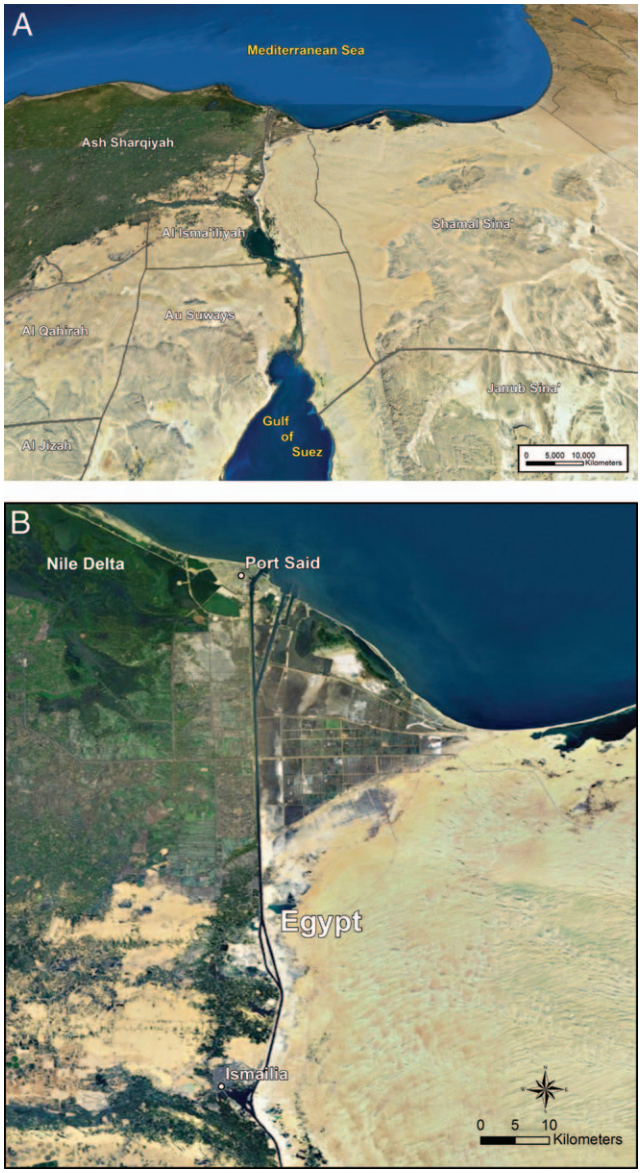

Figure 1. Location of the Suez Canal, Egypt, showing the overall setting of the study region and position of the excavated channel between the Mediterranean Sea and the Red Sea. (A) The Suez Canal lies on the eastern flanks of the Nile Delta and is susceptible to tsunamis originating in the eastern Mediterranean Sea basin. (Based on ESRI, i-cubed, USDA FSA, USGS, AEX, GeoEye, Getmapping, Aerogrid, and IGP). (B) Close-up of the Suez Canal viewed from above the Red Sea, looking northward toward Port Said on the eastern flanks of the Nile Delta. The north–south trending canal transits mostly desert regions until it reaches the fertile Nile Delta lowlands. The global digital elevation model (ETOPO2) represents gridded (2 × 2 min) elevation and bathymetry for the world. (Data derived from the National Geophysical Data Center's ETOPO2 Global 2′ Elevations data set from September 2001).

waves moving through the Suez Canal proper; (3) the 775-m-long El-Salam Syphon under Suez Canal conveying irrigation water to the Sinai Peninsula, which was completed in 1997 (Mazen and Craig, 1995; Serag and Khedr, 2001); (4) the Suez Canal overhead power-line crossing (29.9° N, 32.5° E) by which twin pylons elevate two 500-kV circuits to the required 152-m clearance above the waterway and have a wire span of about 600 m; and (5) the Suez Canal Bridge (30.8° N, 32.3° E) spanning 404 m and affording a waterway clearance of 70 m, which opened to vehicles during October 2001. Damage to the Ismailia Canal, which conveys freshwater from NW Cairo to the Suez Canal, could also be a macroproblem during posttsunami impact recovery operations (Sultan, Santos, and Helaly, 2011).

Prior tsunami events in the Mediterranean and Red Seas (Table 1) suggest potential impacts on the Suez Canal sometime in the future (*e.g.,* Sørensen *et al.,* 2012). Attention is focused on this important waterway because 12% of all tsunamis worldwide occur in the Mediterranean Sea Basin and, on average, one disastrous tsunami takes place there every century (*e.g.,* Govorushko, 2012). According to Papadopoulos *et al.* (2007) and the International Tsunami Information Centre (2011), there is a significant frequency of tsunami events in the Mediterranean, with 200 tsunamis being recorded over the last five centuries. Over the last four centuries, there have been 15 tsunamis every century around Italy. In 1628 BC, the coasts of the entire eastern Mediterranean were submerged by 60-m-high waves caused by a volcanic eruption on Santorini, a Greek island in the Aegean Sea. Earthquake-induced tsunamis originating near the Greek islands of Rhodes and Crete in AD 365 and 303 destroyed coastal developments as far away as Egypt's Nile Delta, the earlier tsunami killing thousands of people in the city of Alexandria (Galanopoulos, 1960; Pararas-Carayannis, 1992). Geological research and historical records report that many powerful tsunamis have taken the lives of thousands of people over the ages in this region. Because the area is clearly tsunami prone, the Suez Canal and its associated infrastructure are likely vulnerable to long-wave impacts in the future.

Shape and Size of the Canal

Opened to shipping in 1869, its maximum navigational depth was then 8 m. Port Said was constructed by 1871, formed by two breakwaters that extended seaward from the low sandy coast. By 1890, the depth had been increased to 8.5 m. The first coal-fueled ship transited the Suez Canal in 1908, and diesel-powered ships were moving through the waterway by 1912. In 2011, cargo ships bigger than 10,000 gross tons made up about 93% of the world's total capacity. Over time, the increasing length and draft of large vessels promoted a gradual improvement in navigational conditions by enlargement of curves (*i.e.,* lessening of curvatures) and standardization of the waterway's navigable depth.

Although there were narrower channel widths in the past, today the canal averages about 300 m wide with an effective navigation width of about 225 m at an 11-m water depth. The present cross-sectional configuration of the canal is shown in Figure 2.

Sea-Level Rise, Subsidence, and Seismic Jolts

A common perception of change in eustatic sea level is that it will rise, flooding low-lying coastal areas (*e.g.,* Church *et al.,* 2001; IPCC, 2001). Global sea-level rise will eventually affect the canal, requiring the imposition of sea locks to avoid

flooding. While the depressed relief of the Suez Canal corridor is considered to be a part of the ancient Nile River's delta, the delta in its destructive phase (eroding) is now subsiding and tilting to the NE toward the entrance/exit at Ports Said and Fouad (Coutellier and Stanley, 1987; Frihy, 2003; Stanley, 1990; Stanley and Warne, 1998; Stanley, McRea, and Waldron, 1996).

In addition to subsidence and erosion of the delta, a second noteworthy macroproblem is the possibility of seismic jolts along the Suez–Cairo–Alexandria shear fault zone (Elenean, Mohamed, and Hussein, 2010). Well-documented 21st-century earthquakes took place there on 29 June 2000, 7 July 2005, and 30 October 2007. Faults, shear zones, and lineament swarms making up part of the tectonic pattern in NE Egypt contribute to seismic risks that could adversely affect the integrity of the canal *per se* (*e.g.,* El-Sayed, Korrat, and Hussein, 2004; Neev, 1977; Neev and Friedman, 1978; Neev, Hall, and Saul, 1982). Earthquakes in the eastern Mediterranean Sea in the recorded past caused tsunami run-ups on Egypt's coastline (*e.g.,* Ambraseys, 1962, 2001; Eckert *et al.,* 2011; Sintubin, 2011), so there is no hesitancy to assume more temblors as a cause of tsunamis hitting the training jetties and navigational channel of the approaches to the Suez Canal at Port Said–Port Fouad.

At the other end of the Suez Canal, on the Red Sea (Figure 1A), paleotsunami deposits have been studied by Salem (2009), who found large carbonate blocks in the carbonate rock sequence alongshore. He reported that beaches on the Red Sea were subjected to paleotsunami waves due to seismic activity inside the Red Sea Basin (Gulf of Suez). His observation of paleoliquefaction and landslides was interpreted as proof that the region has been subjected to strong earthquakes related to rifting. Evidence of volcanic activity at the southern end of the Red Sea is found in Perim Island (an eroded fragment of the SW flank of a volcano from the late Miocene, 10.5 ± 1.0 million years ago) and younger Holocene islands such as Jebel at Tair and the Zubair islands (*e.g.,* Wiart and Oppenheimer, 1999). Jebel at Tair is the northernmost known Holocene volcano in the Red Sea, with explosive eruptions reported in the 18th and 19th centuries. With historical explosive activity reported from the Zubair islands in the 19th century, it is possible that volcanism and associated earthquakes pose a tsunami threat in this region. Thus, during 19–23 December 2011, a new lava-formed island was observed near the Zubair archipelago, possibly indicating volcanic activity is increasing in the basin of the Red Sea.

METHODS

The main procedures used to consider potential impacts of tsunamis on the Suez Canal focus on geological, historical, archeoseismological, and anecdotal data. The general bathymetric map of the eastern Mediterranean Sea shown in Figure 3 highlights the comparatively shallow waters on the continental shelf in the vicinity of the subsiding Nile Delta (*e.g.,* Syvitski *et al.,* 2009). Here, water depths are shallow over the offshore prodelta and to the east offshore from the entrances of the Suez Canal, in the vicinity of Ports Said and Fouad. The concave seaward configuration of the coastline in plan view on the eastern flanks of the Nile Delta and its shallow water depths contribute to wave diffraction and refraction, leading to increased heights of earthquake-induced long waves. The bathymetry also shows unobstructed deep-water approaches to the Port Said–Port Fouad infrastructure.

Perusal of Figure 4 shows that earthquakes (Figure 4A) and volcanic eruptions (Figure 4B) may occur almost anywhere throughout the study area, although there are definite concentrations in the region from the Greek islands (Hellenic Arc) to coastal western and southern Turkey to Crete and along the easternmost shores of the Mediterranean Sea. Earthquakes also occur in and around the Red Sea, while volcanic eruptions are recorded along the eastern margin of the Red Sea in western Saudi Arabia and southern Syria. According to Soloviev (1990), earthquakes are expected to cause 75% of the tsunami events in the Mediterranean Sea. Although there is the possibility of tsunami impacts originating in the Red Sea, this discussion focuses mostly on the Mediterranean Sea because there is much more data available in the form of tsunami catalogues, historical–archeological records, and drill core logs.

TECTONIC SETTING OF THE SUEZ CANAL AND ENVIRONS

Due to active lithospheric tectonic plate convergence, the Mediterranean Sea region is geodynamically characterized by high seismicity and significant volcanism (*e.g.,* Papadopoulos and Fokaefs, 2005). Tsunamigenesis in the Mediterranean Sea Basin is related to complex tectonics that is generally described within the purview of the collision between the Eurasian and the African tectonic plates, as summarized by Tinti *et al.* (2005) for different expressions in various parts of the Mediterranean Sea. The major fault and shear zones around the eastern Mediterranean Sea Basin include the Hellenic Arc, North Anatolian Fault Zone, East Anatolian Fault Zone, Cyprus Arc, Pelusium (megashear) Line, and Dead Sea Fault (*e.g.,* Neev, 1977; Neev, Hall, and Saul, 1982; Yalçiner *et al.,* 2007; Zaytsev *et al.,* 2008). Figure 5 is an example of some major tectonic elements in the general Suez region. Based on extractions from Neev's (1975) maps, Figure 5 shows the Pelusium Line crossing the canal and other major faults in the area that could be sources of earthquake activity. Along the Dead Sea transform (DST) tectonic plate boundary, Girdler (1990), as discussed in Butler and Spencer (1999), points out that present-day seismicity is strongly focused on the Roum Fault, which bypasses the much larger Yammouneh Fault that has been largely inactive over the last 5 million years and which lies closer to the coast than the main transform boundary. A series of volcanic systems occurs at the center of the Aegean Sea that nearly parallels the trench and thus forms an internal arc (Milos, Antimilos, Antiparos, Santorini, Christiana, Colombus, Kos, Yali, Nisiros, *etc.*). Any of these ruptures or volcanic systems constitutes a potential source of tsunamigenesis.

Because seismicity in the Mediterranean Basin is strongly connected to tectonic features and because tsunamis are mostly generated by earthquakes, the geographical distribution of historical tsunamis in the region generally resembles the trend of seismicity. Due to tectonic activity in the eastern Mediterranean Basin, there is a substantial geohazard in this zone

Table 1. *Catalogue of known tsunami events in the east Mediterranean Sea (Greece and surrounding regions, Marmara Sea, Cyprus, and Levantine Sea), 426 BC to AD 2002. (Modified from Papadopoulos and Fokaefs, 2005).*

Year	Month	Day	Region	Reference*	*K*†	*h*‡
−426	Summer		Maliakos Gulf, E Greek mainland	P	8	
−373	Winter		W Corinth Gulf, central Greece	P	9	
66			S Crete	P	4	
142/144			Rhodes island, SE Aegean Sea	PF	7	
365	7	21	Crete island	P	10	
447	1	26	Marmara Sea	P	8	
478	9	25	Marmara Sea	P	7	
544			Thrace, NE Greek mainland	P	8	
551	7	9	Lebanon	PF	8	
552	5		Maliakos Gulf, E Greek mainland	P	8	
556			Cos island, SE Aegean Sea	P	8	
740	10	26	Marmara Sea	P	6	
749	1	18	Levantine Coast	PF	7	
1202	5	20	Syrian Coast and Cyprus	A	7	
1265	8	10	Marmara Sea	P	5	
1270	3		N Ionian Sea	P	5	
1303	8	8	Crete island	P	10	
1343	10	18	Marmara Sea	PF	6	200
1389	3	20	Chios island, E Aegean Sea	P	6	
1402	6		Corinth Gulf, central Greece	P	8	
1419	5	25	Marmara Sea	P	5	
1481	5	3	Rhodes island, SE Aegean Sea	PF	7	
1494	7	1	Crete island	P	4	
1509	9	10	Marmara Sea	P	5	600
1609	4		Rhodes island, SE Aegean Sea	P	8	
1612	11	8	Crete island	P	8	
1630	3	9	Kythira island, SE Aegean Sea	P	5	
1633	11	5	Zante island, Ionian Sea	P	5	
1650	10	11	Thera island, S Aegean Sea	P	10	2000
1667	4	6	S Adriatic Sea	P	5	
1741	1	31	Rhodes island, SE Aegean Sea	P	8	
1742	2	21	W Corinth Gulf, central Greece	P	5	
1748	5	25	W Corinth Gulf, central Greece	P	9	1000
1759	11	25	Akko, Israel	PF	8	
1766	5	22	Marmara Sea	P	7	
1769			E Corinth Gulf, central Greece	P	3	
1772	11	24	Foca, E Aegean Sea	P	5	
1778	6	16	Smyrna, E Aegean Sea	P	5	
1791	11	2	Zante island, Ionian Sea	P	4	
1794	6	11	Central Corinth Gulf	P	5	300
1817	8	23	W Corinth Gulf, central Greece	P	8	500
1833	1	19	Albania	P	5	
1851	10	12	Avlona, Albania	P	4	
1852	9	8	Smyrna, E Aegean Sea	P	4	
1853	8	18	S Evoikos Gulf, E Greek mainland	P	4	
1856	11	13	Chios island, E Aegean Sea	P	8	
1861	12	26	W Corinth Gulf, central Greece	P	5	210
1866	1	2	Albania	P	7	
1866	2	2	Chios island, E Aegean Sea	P	4	
1866	2	6	Kythira island, SE Aegean Sea	P	6	800
1866	3	2	Avlona, Albania	P	4	
1866	3	6	Albania	P	7	
1866	3	13	Albania	P	4	
1867	2	4	Ionian Sea	P	3	
1867	9	9	Gythion, S Greek mainland	P	7	
1869	12	28	Avlona, Albania	P	4	
1878	4	19	Marmara Sea	P	5	
1881	4	3	Chios island, E Aegean Sea	P	4	
1883	6	27	N Aegean Sea	P	4	
1886	8	27	S Ionian Sea	P	4	
1887	10	3	Central Corinth Gulf	P	3	
1888	90	9	Central Corinth Gulf	P	3	
1893	2	9	N Aegean Sea	P	4	100
1893	4	17	Zante island, Ionian Sea	P	3	
1893	6	14	Avlona, Albania	P	4	
1894	4	27	N Evoikos Gulf, E Greek mainland	P	3	

Table 1. *Continued.*

Year	Month	Day	Region	Reference*	*K*†	*h*‡
1894	7	10	Marmara Sea	P	6	
1898	6	2	Corinth Gulf, central Greece	P	4	
1899	1	22	S Ionian Sea	P	4	100
1902	7	5	Thermaikos Gulf, NW Aegean Sea	P	3	
1905	1	20	Magnesia, E Greek mainland	P	3	
1911	2	18	Ochrida Lake, S Yugoslavia	P	3	
1914	11	27	Lefkada island, Ionian Sea	PF	2	300
1914	11	27	Lefkada island, Ionian Sea	PF	5	
1920	11	26	Saseno, Albania	P	5	
1926	8	30	Argolikos Gulf, SW Aegean Sea	P	3	
1928	3	31	Smyrna, E Aegean Sea	P	3	
1932	9	26	Strymonikos Gulf, N Aegean Sea	P	4	200
1947	10	6	S Ionian Sea	P	3	
1948	2	9	Karpathos island, SE Aegean Sea	P	7	400
1948	4	22	Lefkada island, Ionian Sea	P	4	100
1949	7	23	Chios island, E Aegean Sea	P	4	200
1953	8	12	Kefalonia island, Ionian Sea	P	3	
1955	4	19	Volos Gulf, E Greek mainland	P	4	
1956	7	9	Cyclades, S Aegean Sea	PF	8	1500
1962	5	28	Lemnos island, NE Aegean Sea	P	3	
1963	2	7	W Corinth Gulf, central Greece	P	7	500
1965	7	6	W Corinth Gulf, central Greece	P	5	300
1968	2	19	Lemnos island, NE Aegean Sea	P	3	
1979	4	15	Montenegro	P	7	
1981	2	24	E Corinth Gulf, central Greece	P	3	30
1983	1	17	Kefalonia island, Ionian Sea	P	3	50
1984	2	11	W Corinth Gulf, central Greece	P	4	
1991	1	4	Ikaria island, E Aegean Sea	P	3	
1991	5	7	Leros island, E Aegean Sea	P	4	50
1995	6	15	W Corinth Gulf, central Greece	P	4	100
1996	1	1	W Corinth Gulf, central Greece	P	4	200
1999	8	17	Marmara Sea	P	6	250
2000	4	5	Heraklion, N Crete island	P	3	50
2002	26	3	Rhodes island, SE Aegean Sea	N	5	200

* Sources of information compiled from A = Ambraseys (1962), P = Papadopoulos (2001), PF = Papadopoulos and Fokaefs (2005), and N = new observations collected by G.A. Papadopoulos during a postevent field survey, by Papadopoulos and Fokaefs (2005).
† Tsunami intensity as determined by Papadopoulos and Fokaefs (2005), according to the Papadopoulos–Imamura 12-point scale.
‡ h = maximum wave height (amplitude) at the seacoast.

(Papadopoulos *et al.,* 2007; Sørensen *et al.,* 2012; Tarek, Seleem, and Aboulela, 2011). With their ancient civilization, the Greeks compiled one of the longest historical records of earthquakes and tsunamis. This highly active tectonic setting is the *raison d'être* for considering the possibility of tsunami generation and possible impacts along the eastern flanks of the Nile Delta on which entrances to the canal are situated.

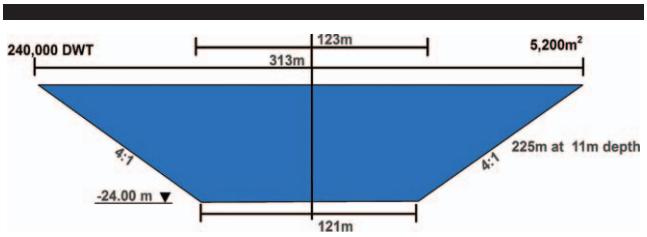

Figure 2. Cross-section of the Suez Canal showing major dimensions *ca.* 2010 with a surface width of 313 m, a basal width of 121 m, and an effective navigational width of 225 m at an 11-m depth that allows passage of a typical Suezmax vessel. The present configuration of the canal is the shape of a waterway that would accommodate the incursion of a tsunami, breaking wave front, and flood wave. (See Figure 7 for further explanation. Based on a diagram from the Suez Canal Authority's Web site).

GENERATION OF TSUNAMIS

In addition to earthquakes and volcanic eruptions, submarine landslides, slumps, and subsidence are responsible for the generation of tsunamis (*e.g.,* Altinok *et al.,* 2011; Parker, 2010; Yalçiner *et al.,* 2002). Landslide tsunamis have smaller horizontal scales than tsunamis generated by earthquakes because they attenuate quickly due to dispersion (Gonzalez and Kulikov, 1993; Mirchina and Pelinovsky, 1988; Torsvik *et al.,* 2010). In addition, theoretical investigations and laboratory computer modeling (*e.g.,* Fine *et al.,* 2003) indicate that submarine landslides are less effective tsunami-generating forces than subaerial landslides entering a body of water. A rigid-body slide produces much higher tsunami waves than a viscous (water-saturated) material slide, a result confirmed by Harbitz *et al.* (2006). Because only a limited part of the potential energy released by the landslide is transferred to the long-wave energy, the critical parameter determining the generation of surface waves is the Froude number (Fr), the

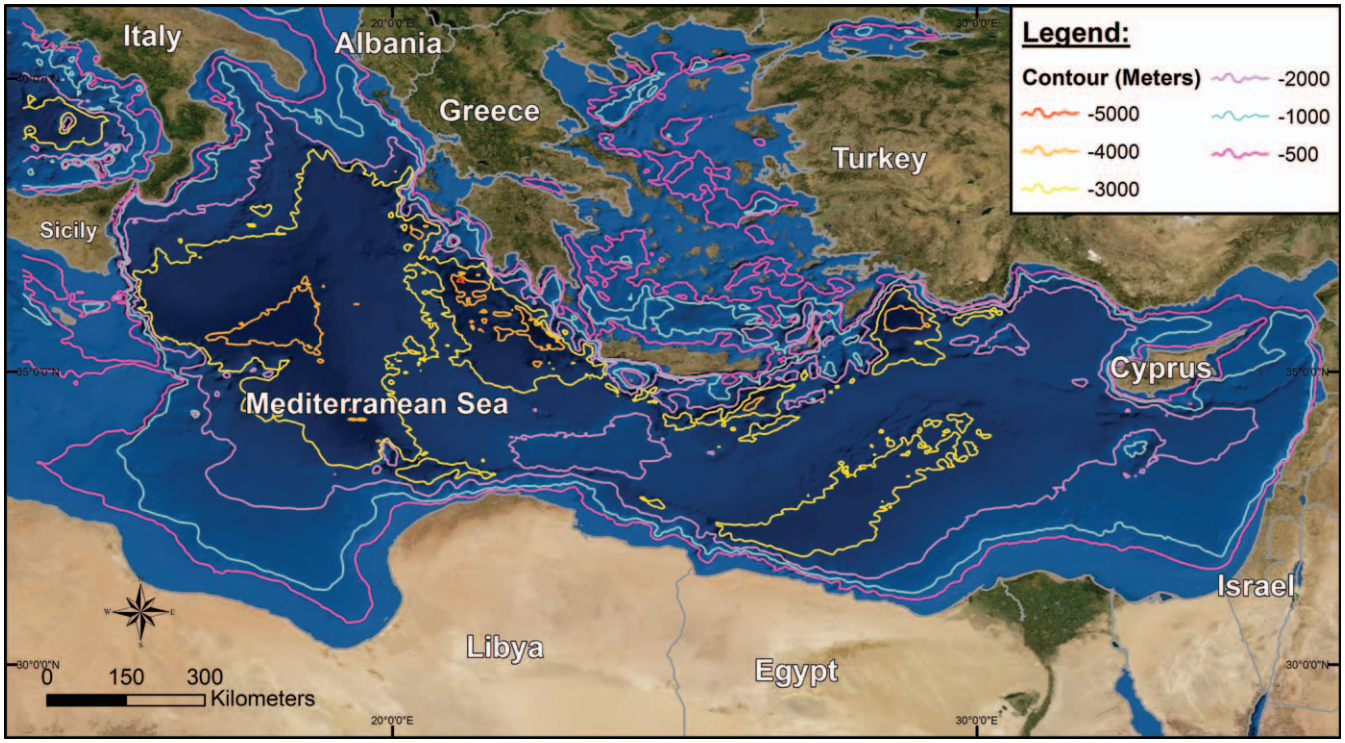

Figure 3. General bathymetry of the eastern Mediterranean Sea showing the proximity of the 500-m isobaths at various locations along the shore. Note the occurrence of shallower waters offshore the Nile Delta and the wider shelf area along the eastern shore of Egypt (Sinai Desert), where the impacts of tsunami wave run-up could be significantly enhanced. ETOPO2 represents gridded (2 × 2 min) elevation and bathymetry for the world. (Data derived from the National Geophysical Data Center's ETOPO2 Global 2′ Elevations data set from September 2001).

ratio between slide and wave velocity, where the most efficient generation occurs near resonance when Fr = 1.0. Subaerial slides displace a considerable volume of seawater at relatively high velocity as they slide into the water from the slope, causing a long wave to form and to radially propagate outward from the impact site.

THE PAST AS A KEY TO THE FUTURE

The methodology discussed here is predicated neither on our interpretations of tsunamigenesis nor on our computer modeling of tsunami wave transmission, although other researchers' efforts at simulations of numerical tsunami propagation are reported (*e.g.,* Beisel *et al.,* 2009; Fine *et al.,* 2003; Salamon *et al.,* 2008; Sintubin, 2011; Sørensen *et al.,* 2012; Yalçiner *et al.,* 2007; Zaytsev *et al.,* 2008). Instead, our analyses depend on an approach that integrates known facts or documented events that are believed to have taken place in the past, even though archeoseismological data and other kinds of interpretations of geological events may not be in perfect agreement. Examination of tsunami catalogues and electronic databases compiled by earlier researchers (*e.g.,* Ambraseys, 1962, 2001; Ambraseys, Melville, and Adams, 2005; Antonopoulos, 1979, 1980; Galanopoulos, 1960; Papadopoulos, 2001; Papadopoulos and Chalkis, 1984; Papadopoulos and Fokaefs, 2005; Papadopoulos *et al.,* 2007; Papazachos *et al.,* 1986; Soloviev *et al.,* 2010) is of great importance to geohazard assessment and especially to our interpretation of potential impacts to the Suez Canal.

Appreciation of prior high-energy events associated with earthquakes, volcanic eruptions, and landslides or undersea slumps that produced tsunamis in the eastern Mediterranean Sea are seen as precursors for similar hydrogeophysical events that could occur in the 21st century. In a sense, we are applying an adaptation of an old geological dictum that the past is a key to the future (Mathieson, 2002), and it is in this sense that we briefly build the case showing that prior tsunamis, however generated, could today threaten the Suez Canal because of repetitious event continuums in the Mediterranean and Red Seas.

TSUNAMI CATALOGUES AND ZONES OF TSUNAMIGENESIS

The eastern Mediterranean Basin is one of the most seismically active and rapidly deforming geodynamic regions in the world (Taymaz, Tan, and Yolsal, 2008), caused by complex geodynamics of continental collision that involves strike-slip faulting, tectonic plate subduction, and crustal extension, as well as volcanism, intense seismic activity, and geomorphological events associated with tsunamis. The complicated tectonic setting of Greece is dominated by the subduction of the African lithosphere beneath the Eurasian Plate along the Hellenic Arc, which consists of an outer

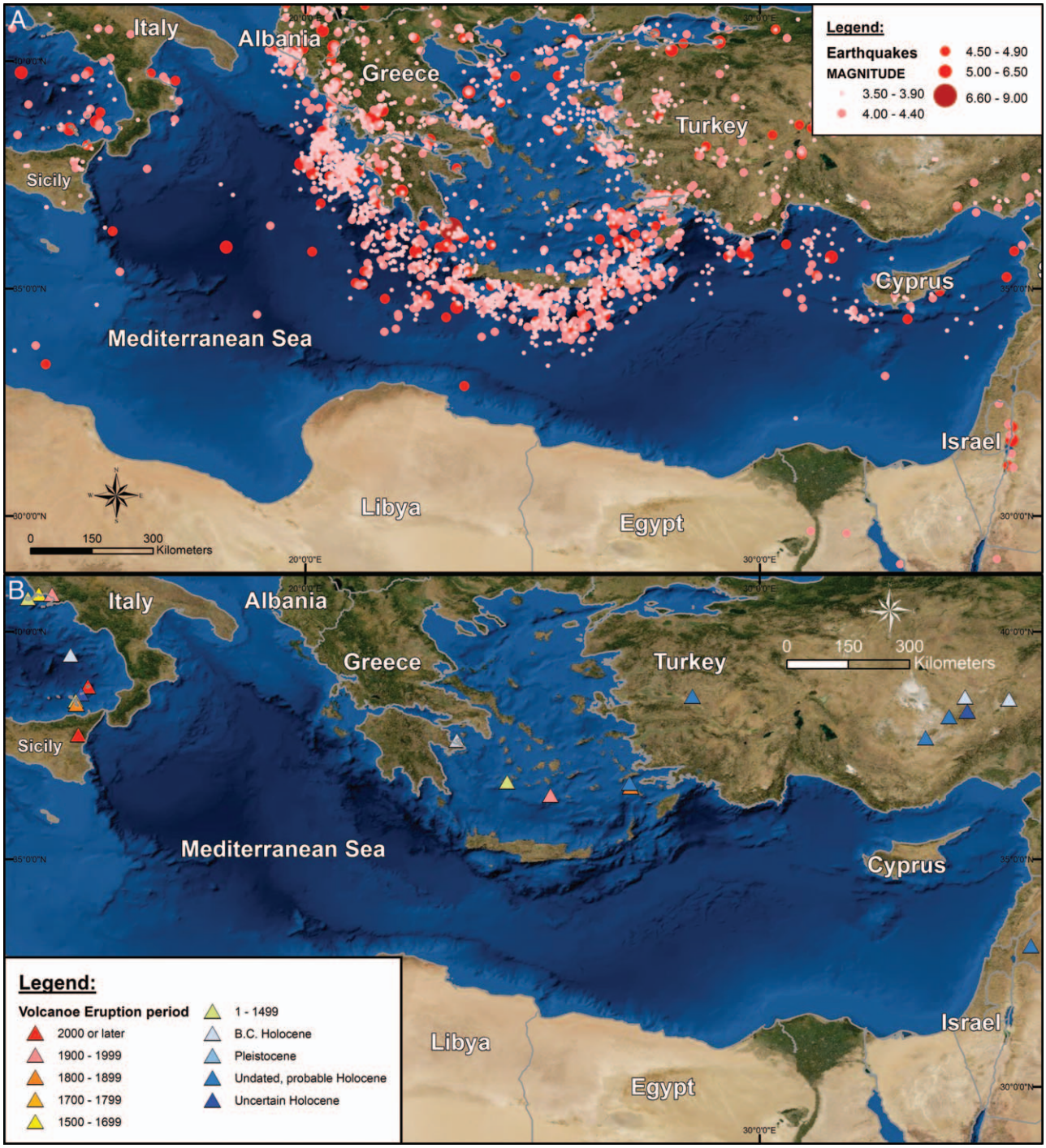

Figure 4. Locations of recorded earthquakes and volcanic activity in the eastern Mediterranean area. (A) Locations of some magnitude 3.9 to magnitude 4.4. temblors N and NW of the N entrance to the Suez Canal. Large, magnitude 4.9 to magnitude 6.5 quakes also occur in the area, posing threats of seismic sea waves that could enter the canal from the Mediterranean Sea or Red Sea. (Earthquake source data from U.S. Geological Survey, 2008, for the period 2004–2007, and background imagery based on ESRI, i-cubed, USDA FSA, USGS, AEX, GeoEye, Getmapping, Aerogrid, and IGP). (B) Volcanic activity in the vicinity of the Mediterranean Sea showing times when there were major eruptions. (Volcano data from the Smithsonian Institution's Global Volcanism Program Web site, and background imagery based on ESRI, i-cubed, USDA FSA, USGS, AEX, GeoEye, Getmapping, Aerogrid, and IGP).

Figure 5. Generalized regional tectonic setting of the Suez Canal, showing some major tectonic elements. The Pelusium Line, which has functioned mostly as a transcurrent fault, lies some 60 km offshore Israel and crosses the Suez Canal south of Port Said, passing along the SE flanks of the Nile Delta and into the Western Desert of Egypt. Some major faults on land and offshore, as well as the axes of major uplifts and coastal hinge lines, are indicated as features that contribute to tectonic instability in the region. (Based on a more detailed map by Neev, 1975).

sedimentary arc and an inner volcanic arc (see the discussion in Papazachos, 1996; Papazachos *et al.,* 2006). The Hellenic Arc is bounded on its NW and E margins by two major transform faults, known as the Cephalonia (right lateral) and the Rhodes (left lateral) Transform Faults. Prominent shallow seismicity is associated with the low-angle thrust faults along the Hellenic Arc. Tinti *et al.* (2005) suggested that the infamous AD 21 July 365 earthquake hypocenter, with the highest magnitude (8.3) reported in earthquake catalogues for Greece, was probably located offshore of western Crete along a major thrust fault parallel to the western Hellenic Trench. This earthquake generated a large tsunami that not only impacted western Crete but also is known to have destroyed settlements in the Nile Delta (see Figure 6 for the location of tsunamigenic zones in the Greek islands), as reported by numerous researchers (*e.g.,* Papadopoulos, 2001; Stiros, 2001, 2007; Stiros and Papageorgiou, 2001). Eckert *et al.* (2011) additionally reported that more than 5000 people in Alexandria lost their lives in the tsunami triggered by the earthquake.

Analysis of tsunami catalogues from different parts of the world shows that more than 2000 tsunami events occurred during the past 4000 years, with about 12% of these distributed events taking place in the Mediterranean Sea Basin (Govorushko, 2012). Certain events, such as the eruption of Santorini and the resulting seismic sea waves, are well known in recorded history. Santorini is the most active volcanic center in the South Aegean Volcanic Arc, though what remains today of that island is chiefly a seawater-filled caldera that is still active (Newman *et al.,* 2012). The island is the site of one of the largest Plinian-type

volcanic eruptions in recorded history that occurred in the Late Bronze Age at an estimated 7.1 on the Volcanic Explosivity Index (*e.g.,* Goodman-Tchernov *et al.,* 2009; McCoy and Heiken, 2000). The Minoan eruption (sometimes called the Thera eruption) occurred some 3600 years ago at the height of the Minoan civilization. It is also known that tsunamis affected the coast of northern Africa, and there is archeological evidence of tsunami deposits in the vicinity of Caesarea on the coast of Israel (Goodman-Tchernov *et al.,* 2009; Reinhardt *et al.,* 2006).

Knowledge of tsunamis in the Mediterranean Sea Basin has accumulated in historical records since the ancient Greeks tried to find explanations for these natural events that caused much havoc in the newly civilized world. Antonopoulos (1979, 1980), for example, catalogued the occurrence of tsunamis in the eastern Mediterranean from antiquity to the time of his reports. His catalogue listed the numerous occurrences of tsunamis and helped to lay the foundation for modern research into this physical phenomenon. Following their 1997 catalogue (Soloviev *et al.,* 1997), which covers the period 2000 BC to AD 1991, Soloviev *et al.* (2010) provide a more extensive and updated catalogue of tsunami occurrence in the Mediterranean Sea Basin from 2000 BC to AD 2000, showing that the tsunami geohazard risk is widespread throughout the Mediterranean Sea Basin. The compilation by Soloviev *et al.* (2010) is especially useful because it summarizes disparate previous works into a unified conception that brings together information from numerous previous catalogues, providing modern researchers with a comprehensive database that indicates detailed descriptive catalogues for specific geographical regions.

Based on compilations of about 300 descriptions of tsunamis and related phenomena, several distinct tsunamigenic zones can be identified in the Mediterranean Sea Basin (Figure 6, compiled from Papadopoulos and Fokaefs, 2005). Of the 300 tsunami events reported in the catalogue compiled by Soloviev *et al.* (2010), about 80% were caused by earthquakes, 2% by volcanic eruptions, and 2% by landslides into the ocean. Causes of the other tsunamis remain unknown.

As far as the SE coasts of the Mediterranean Sea basin are concerned, and especially Egypt's Nile Delta, tsunamis can be generated in several proximal and distal areas where sea waves could enter the canal (see Figure 6 of this paper and, *e.g.,* Figure 1 of Goodman-Tchernov *et al.,* 2009).

According to Ambraseys, Melville, and Adams (2005); Shaw *et al.* (2008); Stiros (2001); and others, a quake of magnitude 8 to 8.5 struck Alexandria on AD 21 July 365, claiming the lives of thousands of local people. The tsunami resulting from this earthquake, causing much destruction in Alexandria, also flooded coastal regions from the Nile Delta to Dubrovnik (Croatia).

Particularly dangerous is the presence of a tsunamigenic zone that lies only 200 km NE from Ports Said and Fouad. Tsunamis generated in this region could easily overtop channel jetties and other shore-protection structures (*e.g.,* bulkheads and revetments) and enter the canal. Approach angles of the long waves are crucial and depend on many variables that are unknowable at the present time, but the substantial point is that the channels and jetties are oriented in a general NE direction and thus face potential wave fronts (see insert in Figure 7). Figures 6 and 7 are thus instructive because they visually demonstrate vulnerability of the canal's northern entrances to tsunamis originating in the eastern Mediterranean Sea.

TSUNAMI FREQUENCY OF OCCURRENCE

The catalogue by Soloviev *et al.* (2010), showing the frequency of occurrence by geographic area, indicates that the return period for sea-wave repetition is about every 10 years for the Aegean Sea, western Greece, and the Calabrian Arc; about 20 to 25 years for Albania, the Dalmatian Coast, and the Ligurian Sea; about every 50 years for eastern Italy and western Italy (the Tyrrhenian Sea); and about every 100 years for the Sea of Marmara, the Near East, and Spain. Based on the two historical tsunami impacts in Alexandria, Eckert *et al.* (2011) estimated a rough frequency of one tsunami every 800 years. Probabilities of tsunamigenesis in the Mediterranean Sea Basin are relatively high, with the possibility that any particular coastal region could be impacted by long-period waves on decadal or centurial scales or multiples thereof (Parsons, 2004).

Although researchers report that one disastrous tsunami occurs within the Mediterranean Sea Basin about every 100 years, there were no catastrophic events during the 20th century. Complicated fault systems between the Eurasia Plate and the descending African Plate ocean seafloor do not normally generate earthquakes, but a separate fault that comes to the surface closer to the island of Crete is capable of producing rare and very large earthquakes that can set off a gigantic tsunami. Shaw *et al.* (2008) indicated that parts of the fault system that generate major tsunamis may recur once every five millennia but that other segments of the fault may slip on a similar scale every 800 years or so. What is unknown is whether the fault that slipped is unique or whether it is part of many contiguous material patches that may slip in the future. In another study, Scheffers *et al.* (2008) studied geological evidence of five tsunamis that hit Greece in the past 2000 years. Although most were small and local, a large sea wave hit SE Crete, southern Rhodes, western Cyprus, southern Syria, and Acre (in northern Israel) in AD 1303. The tsunami, which was generated in the broad Hellenic Arc, thus affected the eastern Mediterranean Sea Basin and severely impacted the Nile Delta, the eastern flanks of which include the twin entrances to the Suez Canal (*cf.* Figure 6).

Prognosis for 21st Century Tsunami Impacts

The question is whether such extreme sea-wave events could occur today. In answer to that potential geohazard threat, Pareschi, Boschi, and Favalli (2006) provided a partial explanation in their investigation of a volcano avalanche in Sicily 8000 years ago, which triggered a devastating tsunami that rapidly spread across the entire Mediterranean Sea. Developing a computer simulation of the Mount Etna avalanche that sent 25 km^3 of rock and sediment tumbling into the adjacent seawater, they reported that the mountain of rubble crashed into the water at more than 320 kph and triggered an underwater mudslide that flowed for hundreds of kilometers

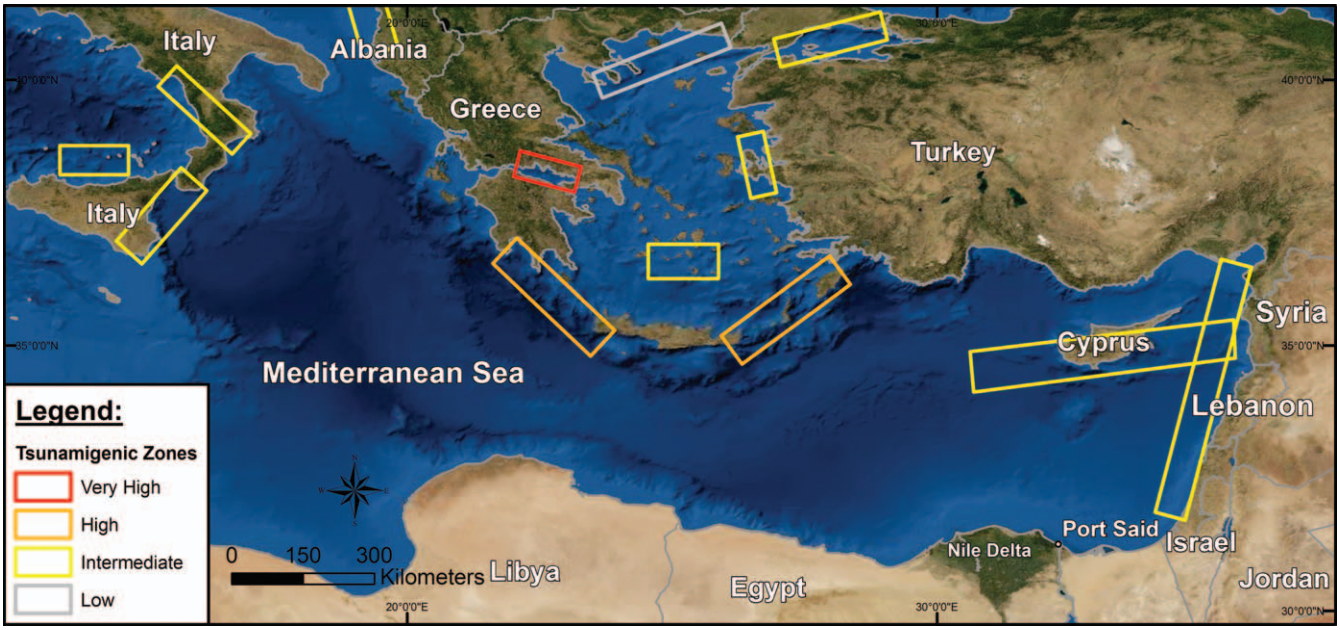

Figure 6. Generalized tsunamigenic zones of the Mediterranean Sea categorized by relative intensity and frequency of occurrence by Papadopoulos and Fokaefs (2005) and showing that the Port Said–Port Fouad harbor complex and entrance to the Suez Canal is most vulnerable to tsunamis of intermediate intensity generated in the Levantine Sea at the eastern end of the Mediterranean Sea Basin and by high-intensity events occurring in the Hellenic Arc. (Modified from Papadopoulos and Fokaefs, 2005). (Background imagery based on ESRI, i-cubed, USDA FSA, USGS, AEX, GeoEye, Getmapping, Aerogrid, and IGP).

undersea. Based on modeling and survey of seafloor sediments displaced by the Mount Etna avalanche, it appears that the tsunami's waves reached heights of 40 m with maximum speeds of 700 kph. The researchers also linked the ancient tsunami with the mysterious abandonment of Atlit-Yam, a Neolithic village on the coast of present-day Israel. According to Pareschi, Boschi, and Favalli (2006), if the same tsunami struck today, southern Italy's seacoast would be inundated within the first 15 minutes. About 1.5 hours later, the seacoast of North Africa, as far east as the city of Benghazi in Libya, would be flooded. After about 3.5 hours, the tsunami would have traversed the entire Mediterranean Sea Basin, passing over and past parts of the Nile Delta to reach the seacoasts of Israel, Lebanon, and Syria.

Goodman-Tchernov *et al.* (2009), studying sedimentary deposits on the continental shelf off Caesarea Maritima, Israel, identified tsunami deposits produced by the Santorini eruption. The deposits were 40 cm in thickness, as found in four cores collected from a 10- to a 20-m water depth. They concluded that the particle-size distribution, planar bedding, shell taphocoenosis, dating (radiocarbon, optically stimulated luminescence, and pottery), and comparison of the horizon with more recent tsunamigenic layers distinguish it from normal storm and typical marine conditions across a wide (>1 km^2) area.

In a similar vein, Cita and Rimoldi (1997) and Cita, Camerlenghi, and Rimoldi (1996) reported that the Santorini eruption produced turbidites and large-volume megaturbidites in the abyssal plains of the Ionian Sea, as well as on the seafloors of small basins of the Mediterranean and Calabrian Ridges. They referred to these bumpy-appearing deposits as "cobblestone topography." This research shows that tsunami waves from the Santorini eruption radiated throughout the eastern Mediterranean, including the Nile Delta, and reached the area where the Suez Canal was eventually constructed by 1869.

MODELS OF POTENTIAL TSUNAMIS, WAVE HEIGHTS, AND WAVE BREAK DISTANCES

Although no computer analyses of potential tsunamis that could impact the eastern Nile Delta, including the two northernmost entrances to the Suez Canal, were conducted, other researchers have initiated mathematical scenarios of interest (*e.g.,* Beisel *et al.,* 2009; Pareschi, Boschi, and Favalli, 2006; Salamon, 2010; Salamon *et al.,* 2008; Sørensen *et al.,* 2012; Tinti *et al.,* 2005; Yalçiner *et al.,* 2007; Zaytsev *et al.,* 2008). Tinti *et al.* (2005), for example, ran several computer simulations, one of which, their "eastern Hellenic Arc scenario," is relevant to a potential tsunami entering the Suez Canal. This scenario regards a thrust force at the eastern end of the Hellenic Arc, with a strike of 300° in front of the SW Turkish coast (*cf.* their Figures 8 and 9). The tsunamigenic force features a magnitude $M_w = 8.0$ and induces maximum positive and negative vertical seafloor deformations of 1.9 and -0.7 m, respectively. This computer simulation predicts that within about 1 hour, the whole eastern Mediterranean Sea coastline would be impacted by the tsunamis generated, with the strongest effects predicted along SW Turkey, Rhodes, the S Aegean and Crete, E Libya, and Egypt. From these analyses,

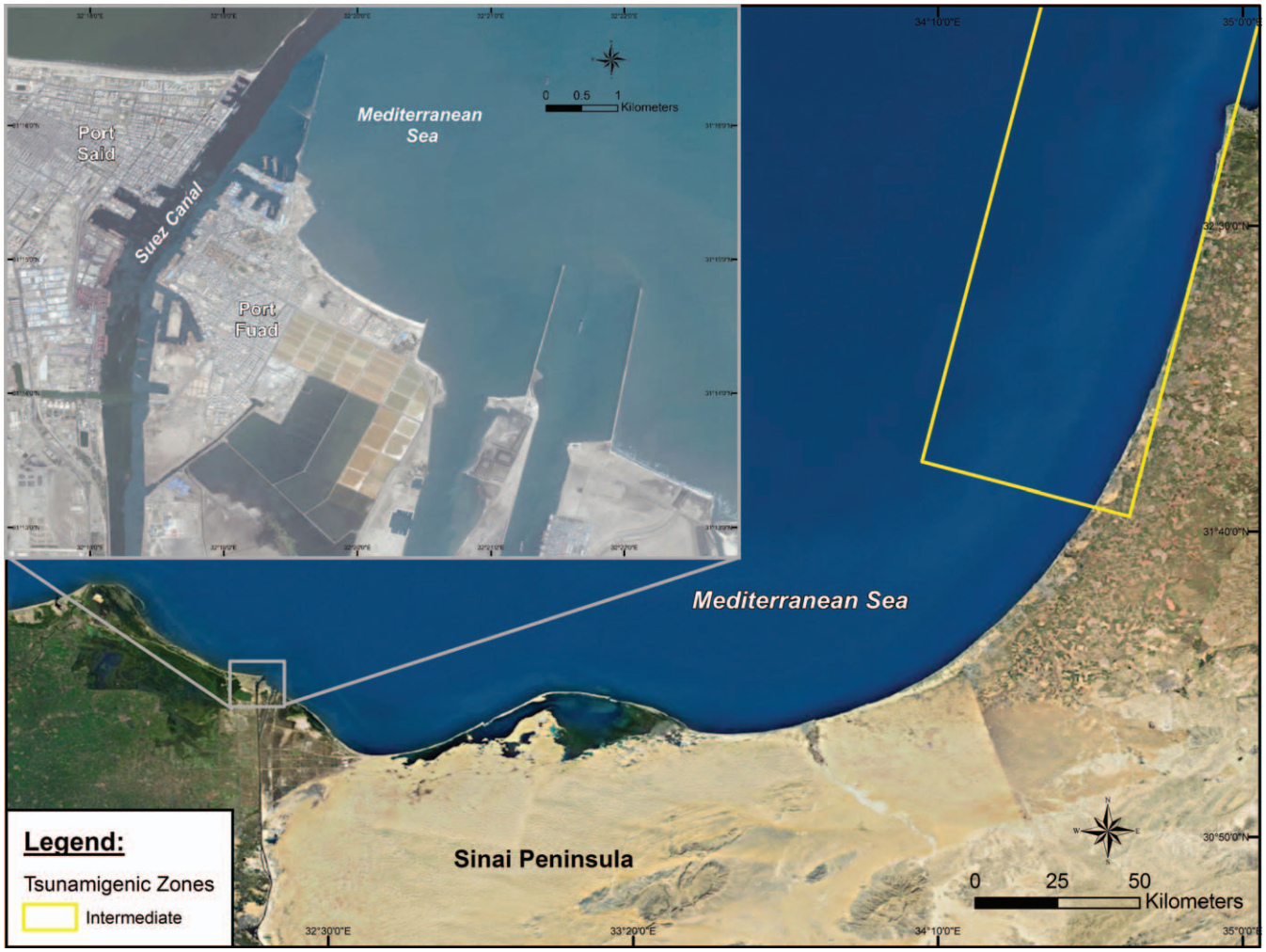

Figure 7. Location of entrances to the Suez Canal on the eastern flank of the Nile Delta, showing the orientation of jetties (detailed insert) in relation to the tsunamigenic zone (yellow box) at the eastern end of the Mediterranean Sea. This earthquake zone, with the potential to produce tsunamis, lies only about 200 km E–NE of the harbor complex. Refer to Figure 5 for a more complete picture of tsunamigenic zones in the eastern Mediterranean Sea Basin. The tsunamigenic zone shown here is based on intensity and frequency of occurrence (as defined by Papadopoulos and Fokaefs, 2005). (Imagery based on ESRI, i-cubed, USDA FSA, USGS, AEX, GeoEye, Getmapping, Aerogrid, IGP, and Google Earth; image date: 3 January 2011).

Tinti *et al.* (2005) found that earthquake-induced tsunamis can be trans–Mediterranean Sea events that affect not only the nearest seacoast but also the remote ones on opposite sides of the basin. Coasts close to the tsunamigenic source are impacted in a very short time (≤15 min), whereas remote seacoasts opposite the source would be flooded within an hour or so.

By applying a Monte Carlo technique, Sørensen *et al.* (2012) were able to provide a probabilistic estimate of earthquake-generated tsunami hazards for the entire Mediterranean Sea. They found that the probability of a tsunami wave exceeding 1 m somewhere in the Mediterranean in the next 30 years was near 100%. Their numerical simulations found the greatest hazards in the eastern Mediterranean because of earthquakes along the Hellenic Arc. Of specific relevance to the Nile Delta and the entrance to the Suez Canal is that the Sørensen *et al.* (2012) models show tsunami hazards concentrated in the eastern Mediterranean with short return periods of 50 years.

In evaluations of tsunami geohazards in the eastern Mediterranean Basin that involved some selected modeling, Salamon *et al.* (2008) reported that many tsunamis in this region appear to have occurred subsequent to onshore earthquakes along the DST, also called the Levant Fault, making it likely that they result from seismogenically induced submarine seabed slides. Areas most affected by the DST fault system include, reading from south to north, the seacoasts of Egypt along the Nile Delta and Sinai, Israel, Lebanon, Syria, and as far north as the Bay of Iskenderun (Alexandretta) in southern Turkey (see Figure 1 of Salamon *et al.,* 2008). After compiling a catalogue of earthquakes and tsunamis, Salamon *et al.* (2008) were able to systematically correlate tsunamis with earthquakes, finding that about 50% of the tsunamis on

the most reliable listing were triggered by local DST earthquakes. According to their integrated list of tsunamis and significant earthquakes in the Eastern Mediterranean Basin, Salamon *et al.* (2008) reported that Alexandria on the Nile Delta had been impacted in 23 ± 3 BC and AD 21 July 365, 8 August 1303, 25 November 1795, 24 June 1870, and 28 December 1908. Eight tsunamis originated from outside the DST system, with four arriving from the Hellenic Arc; however, only the AD 1303 and 1956 tsunamis were reported to have significantly impacted the easternmost Mediterranean shores. Nevertheless, Salamon *et al.* (2008) emphasized that the other two tsunamis, reported only in Alexandria, especially the historical AD 365 tsunami, should not be discounted. These observations suggest that tsunamis along the eastern Mediterranean Sea coast arrive from distant sources and from non-DST sources but that they are not as destructive as the local events, with perhaps the only significant exception being the AD 1303 event. However, the AD 365 Alexandria catastrophe suggests that the Nile Delta is particularly vulnerable.

Shape of a Channeled Tsunami Wave

The previous discussion focused on the potential for tsunami impacts by perusing historical records and reviewing numerical simulations that point to possible impact scenarios for the eastern basin of the Mediterranean Sea. These reviews consider prior known tsunami impacts along the shoreline generally, and especially as they affected the Nile Delta. Relevant to the discussion now is what kind of impact a tsunami would have on the Suez Canal *per se.* To this end, calculations of tsunami wave heights in a fixed channel are thus relevant. General dimensions of the Suez Canal as it now exists (Figure 2) are used for these calculations, assuming a rectangular shape rather than its existing actual trapezoidal form and an effective depth of 24 m.

Usually, when a tsunami (and sometimes a tidal wave) enters a river mouth, it breaks and subsequently propagates as a bore with a steeply sloping front (Chanson, 2011; Tsuji *et al.,* 1991). This configuration of the water waveform is important for ships because, depending on the shape and height of the wave front, the wave threatens safe navigation and controlled ship movement in the canal. Dealing with the problem of a tsunamis-transformed wave entering the canal at either the northern or the southern entrance, we need to consider the characteristic breaking length (distance to the point at which the initially smoothed wave transforms to a breaking wave or bore), which can be found from the formula derived by Zahibo *et al.* (2008)

$$X = \frac{\sqrt{gh}hT}{3\pi a} \qquad (1)$$

where T is the tsunami period, a is the tsunami amplitude, h is channel depth, and g is Earth's gravity acceleration.

A characteristic tsunami period in the world ocean and Mediterranean Sea would be $T = 5$ to 15 minutes, with $a = 2$ to 5 m (*e.g.,* Soloviev *et al.,* 2010). Longer periods of 15 to 40 minutes are usually associated with resonance oscillations of large ocean basins. From a mathematical point of view, the longest waves break over very large distances and resemble surging waves with slow variation in sea level, with weak disturbing action on ships at sea. The effect is more pronounced in a confined space such as a canal. Assuming a Suez Canal channel depth of 24 m, the wave would break from 2 to 10 km down the canal, as shown in Figure 8. Upon entering the canal, the tsunami wave would transform into a bore with a steep, turbulent front at different distances, depending on the wave height.

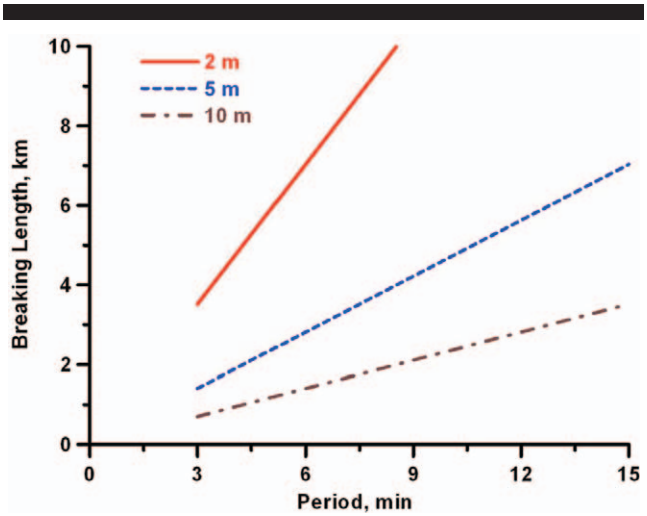

Figure 8. Break points (distance to wave transformation into a bore) of tsunami sea waves entering the Suez Canal versus the tsunami period, showing longer distances down-canal for a 2-m-high wave compared to shorter distances for 5- and 10-m-high breaking waves.

We recognize that the breaking distance (as a wave speed) depends on the shape of the channel, but for qualitative analysis, we did not compute the exact values and instead used calculations for a rectangular channel. The calculation (Figure 8) was based on an uncovered conduit with a rectangular cross-section (*cf.* Figure 2). Didenkulova and Pelinovsky (2011a, 2011b), discussing the influence of channel shape on water wave morphology and attenuation, indicated that the wave shape is modified by conformality to nonrectangular shapes and dimensions. What is important to the topical discussion here is that the magnitude (order) of wave height remains unchanged. This observation is important to safe navigation of ships in the canal because wave surge and height adversely impact the stability of ship traffic. As seen in Figure 8, a 2-m-high long-wave period of about 8 minutes has potential for a nearly 10-km-long (down-canal) break length (distance to transformation). A larger 5-m-high wave with a period of 15 minutes still has a maximum potential break point about 7 km down the canal. A 10-m-high long-wave period of 15 minutes has the potential for doing considerable harm to the harbor and immediately adjacent infrastructure, even with a relatively short break point about 3 km into the canal.

DISCUSSION

The evaluation of potential tsunami impacts on the Suez Canal was based on a review of tsunami catalogues that were compiled by various researchers specializing in tsunamigenic

studies. The timing of many historical tsunamis that were initiated by earthquakes and/or volcanic eruptions is sometimes precisely known (sometimes to the exact day and hour) from recorded history, but the actual degree of total environmental impact largely remains unknown. Historians mainly note that tsunamis caused great damage or simply state without specificity that much of the Nile Delta was annihilated or destroyed. Human deaths were often so numerous that no one remained to tell of the local sea-wave impact event.

The details of such events were not recorded in historical records in the same manner as today, so there is conjecture as to what actually transpired along coastal stretches that experienced massive tsunami run-ups and flooding. Modern knowledge of tsunamigenesis, as related to earthquake intensity and volcanic eruptions, lends credence to some vague ancient reports of the coastal devastation associated with onshore tsunami surges that occurred great distances from source areas (epicenters). The Nile Delta was, for example, likely adversely impacted from tsunamis originating as far away as Sicily and the Greek islands on the opposite side of the eastern Mediterranean Sea. Tsunamis also occurred much closer to the Nile Delta, originating inland from the eastern shore of the Mediterranean Sea. Whatever the source area or tsunamigenic zone, the Nile Delta has been impacted by devastating tsunamis over the last several thousand years.

In other words, paleogeohydrological events usually foreshadow what is yet to come. What is largely unknown is the repetition cycle, because tsunamigenic events may be nonlinear. Whatever the sporadic cyclicity, there is a strong probability that the Suez Canal could be impacted by a tsunami at some point in the future, possibly during the 21st century.

It thus seems prudent to consider some sort of additional protection measure that would mitigate future tsunami impacts. Schuiling *et al.* (2011), for example, suggested the installation of one portable antisurge gate to guard the Suez Canal's Mediterranean Sea opening at the junction of the two entrances/exits (the main canal and the canal's bypass dredged during 1976–80) against incoming Mediterranean tsunamis that might propagate southward inside the main waterway, disrupting ship traffic that is moving, queuing, or moored in the Port Said and Port Fouad harbors (Kaiser, 2009).

The basic macroproject concept is to install movable antisurge gates that exclude seawater waves from entering the Suez Canal. The Netherlands' Maeslant Barrier could serve as a model for needed protection of infrastructure (Schuiling *et al.,* 2011). Surge barriers would not necessarily stop a tsunami but could mitigate some of the strongest adverse impacts along the waterway. As calculated here, long waves of various heights could break 1 to 5 km down-channel, disrupting shipping. Construction of antisurge barriers would thus be a worthwhile macroengineering project of international concern because of the critical need for continued operation of the canal.

CONCLUSION

Our purpose was to outline the vulnerability of the Suez Canal to tsunami attack by chronicling prior disastrous events, *via* the use of tsunami catalogues, and then suggesting the likelihood of repeat performances based on the well-known geophilosophical principle that the past is a key to the future. Specifically, the Panama Canal report of McNamara *et al.* (2011) stimulated this inquiry into the potential effects of tsunamis on the Suez Canal. Papers by Elzeir and Hibino (1999), Alam and Mei (2008), and Yasuda (2010) were also found useful in arriving at our conclusions.

Entrances to the Suez Canal are vulnerable to tsunami impacts along the eastern flanks of the Nile Delta and in the northern Red Sea. Perusal of tsunami catalogues for the Mediterranean Sea Basin shows dangerous tsunamis could impact the Egyptian coast with decadal to centurial frequency (or multiples thereof). Thus, the potential exists for catastrophic future events, only this time the impacts would be greater due to more people living in these coastal areas and the development of widespread industrial and commercial infrastructures. Tsunamigenic regions lie NW of the Port Said and Port Fouad entrances, for example, and historical records show that source areas in southern Italy, Sicily, and the Greek islands have unobstructed trans–Mediterranean Sea transit routes to the Egyptian coast. Even more dangerous is the tsunamigenic region at the eastern end of the Mediterranean Basin that is positioned a few hundred kilometers away, NE of the canal's N entrances. Although there is no definite information as to when a tsunami could impact entrances to the Suez Canal, the available information raises red flags of concern. The construction of channel-guarding barriers should be considered in the interest of geohazard reduction, as well as completion of the Mediterranean tsunami warning system (*e.g.,* Groen *et al.,* 2010; Sørensen *et al.,* 2012) as soon as possible.

ACKNOWLEDGMENTS

We gratefully thank Heather Vollmer (Coastal Education & Research Foundation, West Palm Beach, Florida) for researching remote sensing imagery and geographical information system applications and for preparing the final figures and diagrams for publication. Joanne Bourgeois (Department of Earth and Space Sciences, University of Washington, Seattle, Washington), Jean-Daniel Stanley (Mediterranean Basin Program, Smithsonian Institution, Washington, DC), Paul Komar (College of Earth, Oceanic and Atmospheric Sciences; Oregon State University; Corvallis, Oregon), and Curt Peterson (Department of Geology, Portland State University, Portland, Oregon) are thanked for reviewing an earlier draft of this paper and for making many useful suggestions for improvement.

LITERATURE CITED

Alam, M.-R. and Mei, C.C., 2008. Ships advancing near the critical speed in a shallow channel with randomly uneven bed. *Journal of Fluid Mechanics,* 616, 397–417.

Altinok, Y.; Alpar, B.; Özer, N., and Aykurt, H., 2011. Revision of the tsunamis catalogue affecting the Turkish coasts and surrounding regions. *Natural Hazards and Earth System Sciences,* 11, 273–291.

Ambraseys, N.N., 1962. Data for the investigation of the seismic seawaves in the eastern Mediterranean. *Bulletin of the Seismological Society of America,* 52, 895–913.

Ambraseys, N.N., 2001. Far-field effects of eastern Mediterranean earthquakes in Lower Egypt. *Journal of Seismology,* 5, 263–268.

Ambraseys, N.N.; Melville, C., and Adams, R., 2005. *The Seismicity of Egypt, Arabia and the Red Sea: A Historical Review*. Cambridge, United Kingdom: Cambridge University Press, 204p.

Antonopoulos, J., 1979. Catalogue of tsunamis in the eastern Mediterranean from antiquity to present times. *Annali di Geofisica (Rome),* 32, 113–130.

Antonopoulos, J., 1980. Data from investigation on seismic sea-waves events in the eastern Mediterranean from the birth of Christ to 1980 A.D. *Annali di Geofisica (Rome),* 33(1), 141–248.

Beisel, S.; Chubarov, L.; Didenkulova, I.; Kit, E.; Levin, A.; Pelinovsky, E.; Shokin, Yu., and Sladkevich, M., 2009. The 1956 Greek tsunami recorded at Yafo (Israel) and its numerical modeling. *Journal of Geophysical Research,* 114, C09002.

Butler, R.W.H. and Spencer, S., 1999. Landscape evolution and the preservation of tectonic landforms along the northern Yammouneh Fault, Lebanon. *In:* Smith, B.J.; Whalley, W.B., and Warke, P.A. (eds.), *Uplift, Erosion and Stability: Perspectives on Long-Term Landscape Development*. London: Geological Society, Special Publication No. 162, pp. 143–156.

Calon, J.-P., 1994. The Suez Canal revisited: Ferdinand de Lesseps—the genesis and nurturing of macroengineering projects for the next century. *Interdisciplinary Science Reviews,* 19, 219–230.

Chanson, H., 2011. *Tidal Bores, Aegir, Eagre, Mascaret, Pororoca: Theory and Observations*. New York: World Scientific, 220p.

Church, J.A.; Gregory, J.M.; Huybrechts, P.; Kuhn, M.; Lambeck, K.; Nhuan, M.T.; Qin, D., and Woodworth, P.L., 2001. Changes in sea level. *In:* Houghton, J.T.; Ding, Y.; Griggs, D.J.; Noguer, M.; Van Der Linden, P.J., and Xiaosu, D. (eds.), *Climate Change 2001: The Scientific Basis*. Cambridge, United Kingdom: Cambridge University Press, pp. 639–694.

Cita, M.B. and Rimoldi, B., 1997. Geological and geophysical evidence for a Holocene tsunami deposit in the eastern Mediterranean deep-sea record. *Journal of Geodynamics,* 24(1–4), 293–304.

Cita, M.B.; Camerlenghi, A., and Rimoldi, B., 1996. Deep-sea tsunamis deposits in the eastern Mediterranean: new evidence and depositional models. *Marine Geology,* 104, 155–173.

Coutellier, V. and Stanley, D.J., 1987. Late Quaternary stratigraphy and paleogeography of the eastern Nile Delta, Egypt. *Marine Geology,* 77, 257–275.

Didenkulova, I. and Pelinovsky, E., 2011a. Rogue waves in nonlinear hyperbolic systems (shallow-water framework). *Nonlinearity,* 24, R1–R18.

Didenkulova, I. and Pelinovsky, E., 2011b. Runup of tsunami waves in U-shaped bays. *PAGEOPH,* 168(6–7), 1239–1249.

Eckert, S.; Jelinek, R.; Zeung, G., and Krausmann, E., 2011. Remote sensing–based assessment of tsunami vulnerability and risk in Alexandria, Egypt. *Applied Geography,* 32, 714–723.

Elenean, K.M.A.; Mohamed, A.M.E., and Hussein, H.M., 2010. Source parameters and ground motion of the Suez–Cairo shear zone earthquakes, Eastern Desert, Egypt. *Natural Hazards,* 52, 431–451.

El-Sayed, A.; Korrat, I., and Hussein, H., 2004. Seismicity and seismic hazard in Alexandria (Egypt) and its surroundings. *Pure Applied Geophysics,* 161(5–6), 1003–1019.

Elzeir, M.A. and Hibino, T., 1999. Hydrodynamic simulation of the Suez Canal: a water body connecting two open seas. *Annual Journal of Hydraulic Engineering, JSCE,* 43, 827–832.

Fine, I.V.; Rabinovich, A.B.; Thomson, R.E., and Kulikov, E.A., 2003. Numerical modeling of tsunami generation by submarine and subaerial landslides. *In:* Yalçiner, A.C.; Pelinovsky, E.; Okal, E., and Synolakis, C.E. (eds.), *Submarine Landslides and Tsunamis*. Dordrecht, the Netherlands: Kluwer, pp. 73–93.

Fremaux, C. and Volait, M., 2009. Inventing space in the age of empire: planning experiments and achievements along Suez Canal in Egypt (1859–1956). *Planning Perspectives,* 24, 255–262.

Frihy, O.E., 2003. The Nile Delta–Alexandria coast: vulnerability to sea-level rise, consequences and adaptation. *Mitigation and Adaptation Strategies for Global Change,* 8, 115–138.

Galanopoulos, A.G., 1960. Tsunamis observed on the coasts of Greece from antiquity to present time. *Annali di Geofisica (Rome),* 13, 369–386.

Girdler, R.W., 1990. The Dead Sea transform fault system. *Tectonophysics,* 180, 1–13.

Gonzalez, F.I. and Kulikov, E.A., 1993. Tsunami dispersion observed in the deep ocean. *In:* Tinti, S. (ed.). *Tsunamis in the World*. Dordrecht, the Netherlands: Kluwer, pp. 7–16.

Goodman-Tchernov, B.N.; Dey, H.W.; Reinhardt, E.G.; McCoy, F., and Mart, Y., 2009. Tsunamis waves generated by the Santorini eruption reached eastern Mediterranean shores. *Geology,* 37(10), 943–946.

Govorushko, S.M., 2012. *Natural Processes and Human Impacts: Interactions between Humanity and the Environment*. Dordrecht, the Netherlands: Springer, 14p.

Groen, L.; Joseph, A.; Black, E.; Menictas, M.; Tam, W., and Gabor, M., 2010. Optimal location of tsunamis warning buoys and sea level monitoring stations in the Mediterranean Sea. *Journal of Tsunamis Society International,* 29(2), 78–95.

Harbitz, C.B.; Løvholt, F.; Pedersen, G., and Masson, D.G., 2006. Mechanisms of tsunami generation by submarine landslides: a short review. *Norwegian Journal of Geology,* 86, 255–264.

International Tsunami Information Centre, 2011. Tsunami, The Great Waves. Rome, Italy: UNESCO. http://ioc3.unesco.org/itic/contents.php?id=169.

IPCC (Intergovernmental Panel on Climate Change), 2001. Climate change 2001: the scientific basis. *In:* Houghton, J.T.; Ding, Y.; Griggs, D.J.; Noguer, M.; Van Der Linden, P.J., and Xiaosu, D. (eds.), *Contribution of Working Group I to the Third Assessment Report of the Intergovernmental Panel on Climate Change (IPCC).* Cambridge, United Kingdom: Cambridge University Press, 944p.

Kaiser, M.F., 2009. Environmental changes, remote sensing, and infrastructure development: the case of Egypt's East Port Said harbor. *Applied Geography,* 29, 280–288.

Mathieson, E.L., 2002. The present is the key to the past is the key to the future. *Geological Society of America 98th Annual Meeting, Cordilleran Section, Program and Abstracts, Session 10*. http://gsa.confex.com/gsa/2002CD/finalprogram/abstract_34786.htm.

Mazen, A. and Craig, R., 1995. El Salam Syphon under Suez Canal. *International Journal of Rock Mechanics and Mining Sciences and Geomechanics Abstracts,* 32, 142A.

McCoy, F. and Heiken, G., 2000. Tsunami generated by the Late Bronze Age eruption of Thera (Santorini), Greece. *Pure and Applied Geophysics,* 157, 1227–1256.

McNamara, D.E.; Ringler, A.T.; Hutt, C.R., and Gee, L.S., 2011. Seismically observed seiching in the Panama Canal. *Journal of Geophysical Research,* 116, B04312.

Mirchina, N.R. and Pelinovsky, E.N., 1988. Estimation of underwater eruption energy based on tsunami wave data. *Natural Hazards,* 1(3), 277–283.

Nassar, M.M., 1988. Implications of terrain movements in Egypt. *Journal of Geodynamics,* 10, 73–83.

Neev, D., 1975. Tectonic evolution in the Middle East and Levantine basin (easternmost Mediterranean). *Geology,* 3, 683–686.

Neev, D., 1977. The Pelusium Line: a major transcontinental shear. *Tectonophysics,* 38, T1–T8.

Neev, D. and Friedman, G.M., 1978. Late Holocene tectonic activity along the margins of the Sinai subplate. *Science,* 202(4366), 427–429.

Neev, D.; Hall, J.K., and Saul, J.M., 1982. The Pelusium megashear system across Africa and associated lineament swarms. *Journal of Geophysical Research,* 87(B2), 1015–1030, doi:10.1029/JB087iB02p01015.

Newman, A.V.; Stiros, S.; Feng, L.; Psimoulis, P.; Saltogianni, V.; Jiang, Y.; Papazachos, C.; Karagianni, E., and Vamvakaris, D., 2012. Recent geodetic unrest at Santorini Caldera, Greece. *Geophysical Research Letters,* 39, L06309, doi:10.1029/2012GL051286.

Otsuka, T. and Kamel, I.A., 1995. Rehabilitation of Ahmed Hamdi Tunnel under the Suez Canal: parts 1 and 2. *International Journal of Rock Mechanics and Mining Sciences and Geomechanics Abstracts,* 32, 139A–142A.

Papadopoulos, G.A., 2001. Tsunamis in the east Mediterranean: 1. A catalogue for the area of Greece and adjacent seas. *In: Proceedings of the International Workshop on Tsunami Risk Assessment beyond 2000: Theory, Practice and Plans* (Moscow, Russia, Athens, Greece, National Observatory of Athens, Institute of Geodynamics), pp. 34–42.

Papadopoulos, G.A. and Chalkis, B.J., 1984. Tsunamis observed in Greece and the surrounding area from antiquity to the present times. *Marine Geology,* 56, 309–317.
Papadopoulos, G.A. and Fokaefs, A., 2005. Strong tsunamis in the Mediterranean Sea: a re-evaluation. *ISET Journal of Earthquake Technology,* Paper No. 463, 42(4), 159–170.
Papadopoulos, G.A.; Daskalaki, E.; Fokaefs, A., and Giraleas, N., 2007. Tsunamis hazards in the eastern Mediterranean: strong earthquakes and tsunamis in the East Hellenic arc and trench system. *Natural Hazards and Earth System Sciences,* 7, 57–64.
Papazachos, B.C., 1996. Large seismic faults in the Hellenic Arc. *Annali di Geofisica (Rome),* 39, 891–903.
Papazachos, B.C.; Karakaisas, G.F.; Papazachos, C.B., and Scordilis, E.M., 2006. Perspectives for earthquake prediction in the Mediterranean and contribution to geological observations. *Journal of the Geological Society (London),* Special Publication No. 260, pp. 649–670.
Papazachos, B.C.; Koutitas, Ch.; Hatzidimitriou, P.M.; Karacostas, B.G., and Papaioannou, Ch.A., 1986. Tsunamis hazard in Greece and the surrounding area. *Annales of Geophysics,* 4B(1), 79–90.
Pararas-Carayannis, G., 1992. The tsunami generated from the eruption of the volcano of Santorini in the Bronze Age. *Natural Hazards,* 5, 5–123.
Pareschi, M.T.; Boschi, E., and Favalli, M., 2006. Lost tsunamis. *Geophysical Research Letters,* 33(L22608), 1–6.
Parker, B., 2010. *The Power of the Sea: Tsunamis, Storm Surges, Rogue Waves, and Our Quest to Predict Disasters*. New York: Palgrave Macmillan, 292p.
Parsons, T., 2004. Recalculated probability of M>7 earthquakes beneath the Sea of Marmara, Turkey. *Journal of Geophysical Research,* 109, B05304.
Reinhardt, E.; Goodman, B.; Boyce, J.; Lopez, G.; Hengstum, P.; Rink, W.; Mart, Y., and Raban, A., 2006. The tsunami of 13 December A.D. 115 and the destruction of Herod the Great's harbor at Caesarea Maritima, Israel. *Geology,* 34, 1061–1064.
Salamon, A., 2010. Potential Tsunamigenic Sources in the Eastern Mediterranean and a Decision Matrix for a Tsunamis Early Warning System in Israel. Jerusalem, Israel: Geological Survey of Israel, Report GSI/02/2010, Submitted to the Inter-Ministerial Steering Committee for Earthquake Preparedness, 52p.
Salamon, A.; Rockwell, T.; Ward, S.N.; Guidoboni, E., and Comastri, A., 2008. Tsunami hazard evaluation of the eastern Mediterranean: historical analysis and selected modeling. *Bulletin of the Seismological Society of America,* 97(3), 705–724.
Salem, E.-S.M., 2009. Paleo-tsunami deposits on the Red Sea beach, Egypt. *Arab Journal of Geosciences,* 2, 185–197.
Scheffers, A.; Kelletat, D.; Vött, A.; May, M., and Scheffers, S., 2008. Late Holocene tsunami traces on the western and southern coastlines of the Peloponnesus (Greece). *Earth and Planetary Science Letters,* 269, 271–279.
Schuiling, R.D.; Badescu, V.; Cathcart, R.B.; Seoud, J., and Hanekamp, J.C., 2011. Red Sea heliohydropower: Bab-al-Mandab Sill Macro-Project. *In:* Badescu, V. and Cathcart, R.B. (eds.), *In: Macro-engineering Seawater in Unique Environments: Arid Lowlands and Water Bodies Restoration*. Dordrecht, the Netherlands: Springer, 136p.
Serag, M.S. and Khedr, A.-H.A., 2001. Vegetation–environment relationships along El-Salam Canal, Egypt. *Environmentrics,* 12, 219–232.
Shaw, B.; Ambraseys, N.N.; England, P.C.; Floyd, M.A.; Gorman, G.J.; Higham, T.F.G.; Jackson, J.A.; Nocquet, J.-M.; Pain, C.C., and Piggott, M.D., 2008. Eastern Mediterranean tectonics and tsunamis hazard inferred from the AD 365 earthquake. *Nature Geoscience,* 1(April), 268–276.
Sintubin, M., 2011. Archaeoseismology: past, present and future. *Quaternary International,* 242, 4–10.
Soloviev, S.L., 1990. Tsunamigenic zones in the Mediterranean Sea. *Natural Hazards,* 3, 183–202.
Soloviev, S.L.; Solovieva, O.N.; Go, C.N.; Kim, K.S., and Shchetnikov, N.A., 1997. *Tsunamis in the Mediterranean Sea: 2000 B.C.–1991 A.D*. Moscow: Nauka, 139p [in Russian].
Soloviev, S.L.; Solovieva, O.N.; Go, C.N.; Kim, K.S., and Shchetnikov, N.A., 2010. *Tsunamis in the Mediterranean Sea 2000 B.C.–2000 A.D*. Dordrecht, the Netherlands: Kluwer, 237p.
Sørensen, M.B.; Spada, M.; Babeyko, A.; Wiemer, S., and Grünthal, G., 2012. Probabilistic tsunami hazard in the Mediterranean Sea. *Journal of Geophysical Research,* 117(B1), B01305, doi:10.1029/2010JB008169.
Stanley, D.J., 1990. Recent subsidence and northeast tilting of the Nile Delta, Egypt. *Marine Geology,* 94, 147–154.
Stanley, D.J. and Warne, A.G., 1998. Nile Delta in its destruction phase. *Journal of Coastal Research,* 14, 794–825.
Stanley, D.J.; McRea, J.E., and Waldron, J.C., 1996. *Nile Delta Core and Sample Database for 1985–1994: Mediterranean Basin (MEDIBA) Program*. Washington, DC: Smithsonian Institution, Smithsonian Contributions to the Marine Sciences No. 37, 428p.
Stiros, S.C., 2001. The AD 365 Crete earthquake and possible seismic clustering during the fourth and sixth centuries AD in the eastern Mediterranean: a review of historical and archaeological data. *Journal of Structural Geology,* 23, 545–562.
Stiros, S.C., 2007. Misconceptions for risks of coastal flooding following the excavation of the Suez and the Corinth canals in antiquity. *Mediterranee,* 108, 37–42.
Stiros, S.C. and Papageorgiou, S., 2001. Seismicity of western Crete and the destruction of the town of Kisamos at AD 365: archaeological evidence. *Journal of Seismology,* 5(3), 381–397.
Sultan, S.A.; Santos, F.A.M., and Helaly, A.S., 2011. Integrated geophysical interpretation for the area located at the eastern part of Ismailia Canal, Greater Cairo, Egypt. *Arab Journal of Geoscience,* 4, 735–753.
Syvitski, J.P.M.; Kettner, A.J.; Overeem, I.; Hutton, E.W.H.; Hannon, M.T.; Brakenridge, G.R.; Day, J.; Vorosmarty, C.; Saito, Y.; Giosan, L., and Nicholls, R.J., 2009. Sinking deltas due to human activities. *Nature Geoscience,* 2, 681–686.
Tarek, A.; Seleem, H., and Aboulela, A., 2011. Seismicity and geologic structures indubitable in Wadi Hagul, north Eastern Desert, Egypt. *International Journal of Geosciences,* 2, 55–67
Taymaz, T.; Tan, O., and Yolsal, S., 2008. Recent devastating earthquakes in Turkey and active tectonics of the Aegean and Marmara seas. *In:* Husebye, E.S. (ed.), *Earthquake Monitoring and Seismic Hazard Mitigation in Balkan Countries*. Dordrecht, the Netherlands: Springer, pp. 47–55.
Tinti, S.; Armigliato, A.; Pagnoni, G., and Zaniboni, F., 2005. Scenarios of giant tsunamis of tectonic origin in the Mediterranean. *ISET Journal of Earthquake Technology,* Paper No. 464, 42(4), 171–188.
Torsvik, T.; Paris, R.; Didenkulova, I.; Pelinovsky, E.; Belousov, A., and Belousova, M., 2010. Numerical simulation of tsunami event during the 1996 volcanic eruption in Karymskoe Lake, Kamchatka, Russia. *Natural Hazards and Earth System Sciences,* 10, 2359–2369.
Tsuji, Y.; Yanuma, T.; Murata, I., and Fujiwara, C., 1991. Tsunami ascending in rivers as an undular bore. *Natural Hazards,* 4, 257–266.
Wiart, P. and Oppenheimer, C., 1999. Largest known historical eruption in Africa: Dubbi volcano, Eritrea, 1862. *Geology,* 28, 291–294.
Yalçiner, A.C.; Alpar, B.; Özbay, Y., and Imamura, F., 2002. Tsunamis in the Sea of Marmara: historical documents for the past, models for the future. *Marine Geology,* 190, 445–463.
Yalçiner, A.C.; Pelinovsky, E.; Zaytsev, A.; Kurkin, A.; Ozer, C.; Karakus, H., and Ozyurt, G., 2007. Modeling and visualization of tsunamis: Mediterranean examples. *In:* Kundu, A. (ed.), *Tsunami and Nonlinear Waves*. Dordrecht, the Netherlands: Springer, pp. 273–283.
Yasuda, H., 2010. One-dimensional study on propagation of tsunami wave in river channels. *Journal of Hydraulic Engineering,* 136, 93–105.
Zahibo, N.; Didenkulova, I.; Kurkin, A., and Pelinovsky, E., 2008. Steepness and spectrum of nonlinear deformed shallow water wave. *Ocean Engineering,* 35(1), 47–52.
Zaytsev, A.; Karakus, H.; Yalçiner, A.C.; Chernov, A.; Pelinovsky, E.; Kurkin, A.; Ozer, C.; Dilmen, D.I.; Insel, I., and Ozyurt, G., 2008. Tsunamis in Eastern Mediterranean, histories, Possibilities and Realities. PIANIC-COPEDEC VII (Dubai, UAE), Paper No. 149, pp. 1–10.